

Real-time monitoring of drug release†

Roy Weinstein,^{‡a} Ehud Segal,^{‡b} Ronit Satchi-Fainaro^b and Doron Shabat^{*a}

Received (in Cambridge, UK) 17th September 2009, Accepted 25th November 2009

First published as an Advance Article on the web 10th December 2009

DOI: 10.1039/b919329d

A new prodrug system, assembled using a distinctive coumarin linker, was demonstrated to report real-time activation and drug release *in vitro*.

Drug-delivery systems (DDSs) are being developed to improve the therapeutic index of small molecule drugs.^{1–3} In order to evaluate the therapeutic effect of DDSs, their pharmacokinetics,⁴ pharmacodynamics,⁵ cell permeation efficiencies and pathways,⁶ and mechanisms of activation⁷ are being extensively studied. To date, however, crucial data on time and location of drug release from the delivery system *in vivo*, or even in living cells, cannot be directly obtained. Real-time information on drug release would enable *in vivo* kinetic studies of the release process. Therefore, DDSs that instantaneously report on the release of their active drug could be of great benefit, especially if the reported signal could be detected in a non-invasive manner. Latent fluorophores (LFs) are attractive candidates for this type of reporter.^{8,9} By coupling LF activation to the drug release event in a delivery system, real-time information about the release process can be obtained using non-invasive fluorescence detection techniques. Herein, we describe the design, synthesis and characterization of the first reporting drug-delivery system (RDDS) for *in vitro* use.

The design of our RDDS was based on a 7-hydroxycoumarin linker (compound **4**) with a hydroxymethyl substituent (Fig. 1). The phenolic alcohol of **4** is connected to a triggering group (that can be activated either chemically or enzymatically) and the hydroxymethyl substituent serves as a “handle” for attachment of an end-unit (in this case, the drug).^{10–12} The release of the end-unit is initiated by removal of the trigger of molecule **1** and formation of phenolate **2**. A spontaneous 1,8-elimination¹³ reaction then takes place, leading to the release of the end-unit and generation of coumarin quinone-methide derivative **3**. Addition of a water molecule to the reactive quinone-methide **3** leads to the formation of the highly fluorescent coumarin derivative **4**.

When the trigger of molecule **1** is attached, no fluorescence is emitted.¹⁴ However, when the system undergoes specific activation, the end-unit is released and fluorescence is generated through formation of coumarin **4**. By employing a

drug molecule as the end-unit, such a system can serve as a reporting drug-delivery system. Coupling of the ON–OFF fluorescent signal to the event of drug release provides real-time information about the release process that can be detected by fluorescent imaging techniques in a non-invasive manner. As a model system, we synthesized molecule **5** with a phenylacetamide trigger designed for cleavage by the enzyme penicillin-G-amidase (PGA) and with the chemotherapeutic drug melphalan as the end-unit (Fig. 2). Cleavage of the phenylacetamide moiety by PGA generates an aniline derivative, which undergoes spontaneous 1,6-elimination followed by decarboxylation. The exposed secondary amine then undergoes an intramolecular cyclization to release the phenolate of coumarin. 1,8-Elimination eventually results in the formation of free melphalan and fluorophore **4** (see ESI† for disassembly mechanism).

The release of melphalan from RDDS **5** upon incubation with PGA in PBS (pH 7.4) was monitored by RP-HPLC (Fig. 3A). The fluorescence generated from the linker was monitored using a spectrophotometer ($\lambda_{\text{ex}} = 315 \text{ nm}$, $\lambda_{\text{em}} = 460 \text{ nm}$, Fig. 3B). When RDDS **5** was incubated with PGA, free melphalan was released, accompanied by a gradual increase in fluorescence emitted at 460 nm. In contrast, no melphalan and no fluorescence were observed in the absence of PGA. The observed short time-gap between melphalan release and fluorescence generation is probably due to an additional step required for fluorophore **4** formation (see Fig. 1). These results demonstrate that upon specific activation of RDDS **5**, fluorescent signal is directly correlated to drug release.

With these results in hand, we evaluated both the ability of RDDS **5** to report drug release and the efficacy of the released drug in cells. Human T-lineage acute lymphoblastic leukemia MOLT-3 cells were treated with various concentrations of RDDS **5** in the presence or absence of 1 μM PGA. A colorimetric assay based on tetrazolium salt XTT was used to evaluate cytotoxicity. The data from the cell proliferation assay are presented in Fig. 4A. In the absence of PGA, molecule **5** showed only minor cytotoxicity, even at relatively high concentrations ($\text{IC}_{50} > 100 \mu\text{M}$). However, in the presence of PGA, molecule **5** had cytotoxicity equivalent to

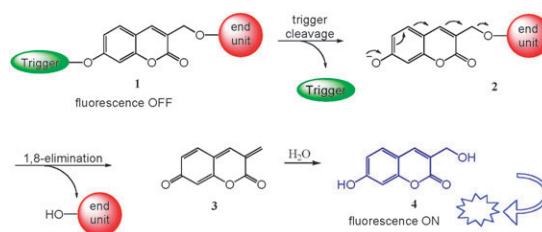


Fig. 1 Proposed disassembly mechanism of coumarin-based RDDS.

^a School of Chemistry, Raymond and Beverly Sackler Faculty of Exact Sciences, Tel-Aviv University, Tel Aviv 69978, Israel. E-mail: chdoron@post.tau.ac.il; Fax: +972 (0)3 640 5761; Tel: +972 (0)3 640 8340

^b Department of Physiology and Pharmacology, Sackler Faculty of Medical Sciences, Tel-Aviv University, Tel Aviv 69978, Israel

† Electronic supplementary information (ESI) available: Experimental details, synthetic schemes, additional supporting data including NMR spectra of all new compounds. See DOI: 10.1039/b919329d

‡ These authors contributed equally.

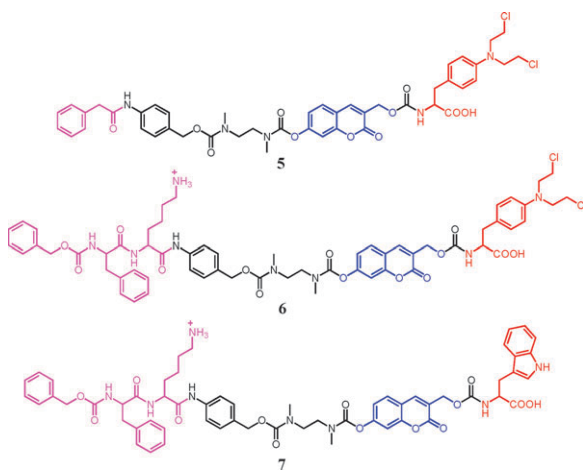


Fig. 2 Chemical structures of synthetic coumarin-based RDDSs.

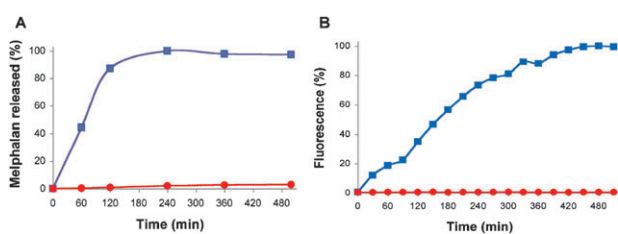


Fig. 3 (A) Melphalan released from RDDS 5 [300 μM] in 100 μL PBS (pH 7.4) in the presence (blue squares) or absence (red circles) of 0.1 mg mL^{-1} PGA. (B) Emitted fluorescence ($\lambda_{\text{ex}} = 315 \text{ nm}$, $\lambda_{\text{em}} = 460 \text{ nm}$) from 300 μM RDDS 5 in 100 μL PBS (pH 7.4) in the presence (blue squares) or absence (red circles) of 0.1 mg mL^{-1} PGA.

that of free melphalan ($\text{IC}_{50} = 2.5 \mu\text{M}$). No cytotoxicity was observed for the linker coumarin 4. The fluorescence emitted from the treated MOLT-3 cells over this same time course was monitored in real-time. The data for MOLT-3 cells treated with 5 μM RDDS 5 and PGA are shown in Fig. 4B. A gradual increase in fluorescence was observed over 1 hour. No increase in fluorescence was observed in the absence of PGA. These results suggest that fluorescence emitted due to drug release from RDDS 5 can be used to monitor growth inhibition activity.

In order to achieve selective activation of a RDDS in cancer cells,¹⁵ we chose the proteolytic enzyme cathepsin B to activate the trigger. This enzyme is a member of the cathepsin family; these proteases are abundant in endosomes and lysosomes.

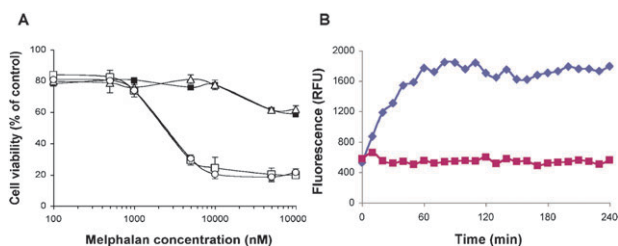


Fig. 4 (A) Viability of leukemia MOLT-3 cells treated with melphalan (\circ), RDDS 5 + PGA [1 μM] (\square), RDDS 5 (\blacksquare), and coumarin 4 (\diamond), at the indicated concentrations in RPMI medium. Cells were incubated for 72 hours. (B) Emitted fluorescence ($\lambda_{\text{ex}} = 315 \text{ nm}$, $\lambda_{\text{em}} = 460 \text{ nm}$) from MOLT-3 cells treated with 5 μM RDDS 5 in the presence (blue diamonds) and absence (red squares) of 1 μM PGA.

Cathepsin B expression is elevated in cancer cells and in tumor endothelial cells,^{16,17} making it useful for prodrug¹⁸ and DDS activation.¹⁹ A low molecular weight RDDS equipped with a suitable trigger can be taken into cells *via* a non-specific pathway, for example through pinocytosis, and will then undergo specific activation by the targeted enzyme in the endolysosomal environment.

To test this approach, we synthesized molecule 6, equipped with the dipeptide Phe-Lys as the triggering-substrate for cathepsin B^{20,21} and melphalan as the end-unit (Fig. 2). Cleavage of the amide bond at the C-terminus of the lysine initiates the disassembly cascade, resulting in the release of free melphalan and the formation of fluorophore 4. Two populations of MOLT-3 cells were subjected to treatment with RDDS 6 in a cell growth inhibition assay. The first was grown in complete medium (RPMI supplemented with 10% fetal bovine serum) before treatment and the other was grown in starvation medium (RPMI supplemented with 2% fetal bovine serum) during the 24 hours prior to treatment. Under these stress conditions, cells are known to increase the expression of proteolytic enzymes.^{22,23} Cell starvation was thus used to mimic the elevated expression of proteolytic enzymes observed in cancerous tissue. When cells were treated with free melphalan, there was no difference in its toxicity between starved or non-starved MOLT-3 cells (data not shown). In contrast, RDDS 6 was more toxic toward the starved cells ($\text{IC}_{50} = 4 \mu\text{M}$) by 7.5 fold than towards non-starved cells ($\text{IC}_{50} = 30 \mu\text{M}$) (Fig. 5A). We presume that the increased cytotoxicity of RDDS 6 towards starved MOLT-3 cells resulted from elevated expression of proteolytic enzymes, including cathepsin B, which specifically activates the RDDS trigger. The fluorescence emitted from the treated MOLT-3 cells was monitored in real-time. The fluorescence signal from starved MOLT-3 cells treated with RDDS 6 was significantly higher than the signal from non-starved cells (see ESI[†]). The strong correlation between cytotoxicity and emitted fluorescence (Fig. 5B) demonstrates the ability of RDDSs, like 6, to report on their activity. In order to determine whether any of the fragments of the RDDS are toxic to the cells, a control experiment was performed with model RDDS 7 (Fig. 2). This model RDDS was equipped with the end-unit tryptophan instead of melphalan and was thus not expected to be toxic. Indeed as shown in Fig. 5A, RDDS 7 was not toxic toward either MOLT-3 population.

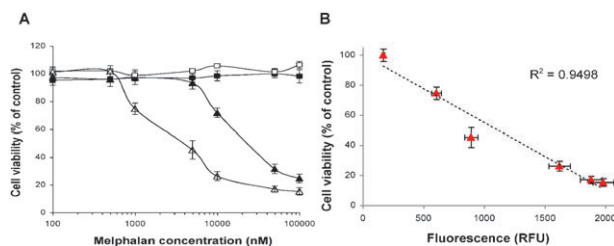


Fig. 5 (A) Viability of non-starved leukemia MOLT-3 cell line treated with RDDS 7 (\blacksquare) or RDDS 6 (\blacktriangle) and starved leukemia MOLT-3 cells treated with RDDS 7 (\square) or RDDS 6 (\triangle). Cells were incubated for 72 hours. (B) Correlation between viability of starved leukemia MOLT-3 cells treated with varying concentrations of RDDS 6 and emitted fluorescence ($\lambda_{\text{ex}} = 315 \text{ nm}$, $\lambda_{\text{em}} = 460 \text{ nm}$).

To further support our conclusions, we monitored the activation of RDDS **6** in human umbilical vein endothelial cells (HUVEC) by confocal microscopy. Cathepsin B has been associated with angiogenesis processes and is observed at high levels in lysosomes of tumor endothelial cells. HUVEC were serum-starved, treated with RDDS **5** or RDDS **6**, then washed, stained, and prepared for microscopy using standard procedures. When HUVEC were treated with RDDS **5**, no coumarin **4** fluorescence was observed, indicating that RDDS **5** is not activated (Fig. 6A–D). This result is consistent with the observed inability of RDDS **5** to inhibit HUVEC growth in a cell proliferation assay (data not shown). In contrast, the confocal images indicated the presence of fluorophore **4** in the HUVEC treated with RDDS **6** (Fig. 6E–H). The location of the coumarin **4** molecules inside the cells was confirmed by confocal Z-stack images (see ESI†). Intracellular coumarin indicates that RDDS **6** molecules were internalized and then were specifically activated by cathepsin B, releasing concomitantly fluorophore **4** and free melphalan. As indicated in the channel overlay (Fig. 6H), HUVEC incubated with RDDS **6** showed cytoplasmic accumulation of activated coumarin.

Although there is a short time-gap between the release of the free drug and the released fluorescence (Fig. 2), the observed signal can be calibrated to report the prodrug activation in real-time. While, there are many examples of DDSs labeled with fluorophores to allow pharmacokinetic evaluation,²⁴ these systems do not report release of the drug from the delivery vehicle. The concept presented in this study describes the first system in which the generation of the active free drug is visualized and reported by a fluorescent signal. The emitted fluorescence of the coumarin linker at a wavelength of 460 nm was sufficient to monitor the DDS activation *in vitro*. However, in order to monitor such DDSs *in vivo*, analogous linkers with fluorescence emitted at longer wavelengths will be required.

In conclusion, we have introduced a novel coumarin-based linker with latent fluorescence into reporting drug-delivery systems. Coupling of latent fluorophore activation with a drug release event resulted in DDSs that report cargo release through an ON–OFF fluorescent signal. We showed that PGA- and cathepsin-B-activated RDDSs signal their cytotoxic

activity toward MOLT-3 cells and HUVEC, respectively, by emitting fluorescence. This allowed us to monitor in real-time the drug release. We observed a strong direct correlation between tumor cell growth inhibition activity and emitted fluorescence in MOLT-3 cells. Using confocal microscopy, we showed that the drug release event in HUVEC occurred in the cytoplasm. The amount of drug release can be calculated by quantifying the emitted fluorescence; this should allow prediction of a DDS's therapeutic effect and potential side effects. Other RDDSs can be similarly designed by introducing appropriate reporting agents and a variety of potent anticancer drugs.

D. S. thanks the Israel Science Foundation (ISF) for financial support and R. W. thanks Ian Seiple from Phil S. Baran's laboratory for helpful discussions.

Notes and references

- M. E. Davis, Z. Chen and D. M. Shin, *Nat. Rev. Drug Discovery*, 2008, **7**, 771–782.
- (a) R. Haag and F. Kratz, *Angew. Chem., Int. Ed.*, 2006, **45**, 1198–1215; (b) D. Shabat, C. Rader, R. A. Lerner and C. F. Barbas, *Proc. Natl. Acad. Sci. U. S. A.*, 1999, **96**, 6925–6930.
- S. H. Medina and M. E. H. El-Sayed, *Chem. Rev.*, 2009, **109**, 3141–3157.
- R. Satchi-Fainaro, M. Puder, J. W. Davies, H. T. Tran, D. A. Sampson, A. K. Greene, G. Corfas and J. Folkman, *Nat. Med.*, 2004, **10**, 255–261.
- Y. Cheng and T. Xu, *Eur. J. Med. Chem.*, 2008, **43**, 2291–2297.
- E. A. Goun, T. H. Pillow, L. R. Jones, J. B. Rothbard and P. A. Wender, *ChemBioChem*, 2006, **7**, 1497–1515.
- R. Satchi-Fainaro, R. Mamluk, L. Wang, S. M. Short, J. A. Nagy, D. Feng, A. M. Dvorak, H. F. Dvorak, M. Puder, D. Mukhopadhyay and J. Folkman, *Cancer Cell*, 2005, **7**, 251–261.
- D. W. Domaille, E. L. Que and C. J. Chang, *Nat. Chem. Biol.*, 2008, **4**, 168–175.
- N. Johnsson and K. Johnsson, *ACS Chem. Biol.*, 2007, **2**, 31–38.
- A. Gopin, N. Pessah, M. Shamis, C. Rader and D. Shabat, *Angew. Chem., Int. Ed.*, 2003, **42**, 327–332.
- A. Gopin, C. Rader and D. Shabat, *Bioorg. Med. Chem.*, 2004, **12**, 1853–1858.
- D. Shabat, R. J. Amir, A. Gopin, N. Pessah and M. Shamis, *Chem.–Eur. J.*, 2004, **10**, 2626–2634.
- M. Shamis and D. Shabat, *Chem.–Eur. J.*, 2007, **13**, 4523–4528.
- E. Leroy, N. Bensel and L. Reymond Jean, *Bioorg. Med. Chem. Lett.*, 2003, **13**, 2105–2108.
- L. Stern, R. Perry, P. Ofek, A. Many, D. Shabat and R. Satchi-Fainaro, *Bioconjugate Chem.*, 2009, **20**, 1783–1791.
- J. A. Foekens, J. Kos, H. A. Peters, M. Krasovec, M. P. Look, N. Cimerman, M. E. Meijer-Van Gelder, S. C. Henzen-Logmans, W. L. J. Van Putten and J. G. M. Klijn, *J. Clin. Oncol.*, 1998, **16**, 1013–1021.
- T. Strojnik, J. Kos, B. Zidanik, R. Golouh and T. Lah, *Clin. Cancer Res.*, 1999, **5**, 559–567.
- S. C. Jeffrey, M. T. Nguyen, J. B. Andreyka, D. L. Meyer, S. O. Doronina and P. D. Senter, *Bioorg. Med. Chem. Lett.*, 2006, **16**, 358–362.
- K. Miller, R. Erez, E. Segal, D. Shabat and R. Satchi-Fainaro, *Angew. Chem., Int. Ed.*, 2009, **48**, 2949–2954.
- G. M. Dubowchik, R. A. Firestone, L. Padilla, D. Willner, S. J. Hofstead, K. Mosure, J. O. Knipe, S. J. Lasch and P. A. Trail, *Bioconjugate Chem.*, 2002, **13**, 855–869.
- M. A. Walker, G. M. Dubowchik, S. J. Hofstead, P. A. Trail and R. A. Firestone, *Bioorg. Med. Chem. Lett.*, 2002, **12**, 217–219.
- C. Cuvier, A. Jang and R. P. Hill, *Clin. Exp. Metastasis*, 1997, **15**, 19–25.
- B. F. Sloane, K. Moin, E. Krepela and J. Rozhin, *Cancer Metastasis Rev.*, 1990, **9**, 333–352.
- A. Agarwal, P. K. Tripathi, S. Tripathi and N. K. Jain, *Curr. Drug Targets*, 2008, **9**, 895–898.

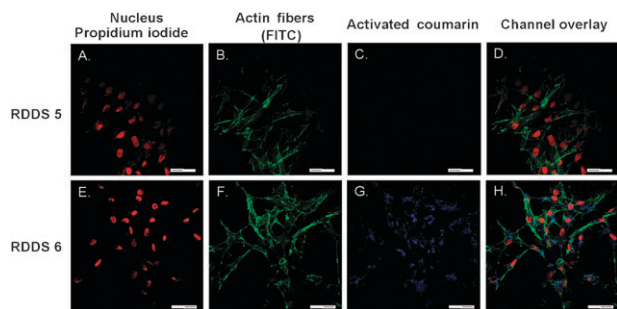


Fig. 6 Subcellular confocal imaging of HUVEC treated with RDDS **5** (panels A–D) and RDDS **6** (panels E–H). HUVEC were incubated with RDDS **5** or RDDS **6** and were fixed and stained with propidium iodide (red) for nuclei and phalloidin-FITC (green) for actin fibers. Activated coumarin (blue) was not detected in HUVEC treated with RDDS **5** but was observed in cells treated with RDDS **6**. Scale bars represent 50 μm .